

# Luminescent properties and concentration quenching mechanism of $\text{Sr}_2\text{B}_2\text{O}_5:\text{xEu}^{2+}$

D. HUANG<sup>a,c</sup>, Q. LIU<sup>b,\*</sup>

<sup>a</sup>State Key Laboratory of Super hard Materials, Jilin University, Changchun, 130022, P. R. China

<sup>b</sup>School of Material Science and Engineering, Changchun University of Science and Technology, Changchun, 130022, P. R. China

<sup>c</sup>Department of Materials Science and Engineering, Jilin Jianzhu University, Changchun, 130022, P. R. China

The  $\text{Sr}_2\text{B}_2\text{O}_5:\text{Eu}^{2+}$  phosphors were synthesized by high-temperature solid state reaction method. The crystal structure of  $\text{Sr}_2\text{B}_2\text{O}_5$ :  $\text{Eu}^{2+}$  is monoclinic system with space group of  $\text{P}2_1/\text{a}(14)$  and the diffraction peaks positions increase slightly with the increase of  $\text{Eu}^{2+}$  doping concentrations. The excitation spectrum locates at UV region and consists of a broad band from 200 nm to 264 nm and a little excitation peak at 355 nm. The emission spectrum of the samples is a broad asymmetric band peaking at 469 nm corresponding to the  $4f^65d^1$  to  $4f^7$  transition of  $\text{Eu}^{2+}$  ion. The best concentration of  $\text{Eu}^{2+}$  ions is 5 mol%. The concentration quenching is caused by the dipole-dipole interaction and radiation re-absorption of  $\text{Eu}^{2+}$  ions.

(Received June 9, 2018; accepted April 8, 2019)

**Keywords:**  $\text{Sr}_2\text{B}_2\text{O}_5$ :  $\text{Eu}^{2+}$ , Phosphor, Luminescence, Concentration quenching

## 1. Introduction

White light-emitting diodes comparing with incandescent light bulbs and fluorescent lamps have many advantages, such as, saving energy, high efficiency, durability, reliability and more switches and long lifetime, etc. [1, 2, 3]. Therefore, white LEDs have been attention as an advanced illumination lighting, and as the fourth generation of illumination technology [4, 5]. In recent decades, white LEDs have been developed rapidly and their properties have made great progress. The method of phosphor conversion has been widely used to prepare white LEDs. For the method, the phosphors have become the key of white LEDs properties. Recently, many common kinds of yellow phosphor materials excited by blue chip, such as YAG [6, 7], sulfides [8, 9], silicates [10, 11], borates [12, 13], nitrides [14] etc. have been studied, and YAG: $\text{Ce}^{3+}$  and  $\text{Sr}_3\text{SiO}_5:\text{Eu}^{2+}$  phosphors have been used widely. Otherwise, various composed and structural borate-based phosphors have lately attracted many people's attention due to its simple preparation, low calcining temperature and high luminous brightness [15, 16, 17]. In 2013, Quansheng Liu et al. reported the crystal structure and luminescent properties of  $\text{Sr}_2\text{B}_2\text{O}_5:\text{Eu}^{2+}$  phosphor [17]. Based on ahead research, we studied the effects of  $\text{Eu}^{2+}$  ions concentration on the structure and luminescent properties of  $\text{Sr}_2\text{B}_2\text{O}_5:\text{Eu}^{2+}$  phosphor, explained the concentration quenching mechanism.

## 2. Experimental

The  $\text{Sr}_2\text{B}_2\text{O}_5:\text{xEu}^{2+}$  phosphors with various  $\text{Eu}^{2+}$  ions concentration were synthesized by high-temperature solid state reaction method. The starting materials used to prepare  $\text{Sr}_2\text{B}_2\text{O}_5:\text{xEu}^{2+}$  phosphors were  $\text{SrCO}_3$  (AR),  $\text{H}_3\text{BO}_3$  (AR), and  $\text{Eu}_2\text{O}_3$  (99.99%). The starting materials were calculated according to the stoichiometric amounts of  $\text{Sr}_{2-x}\text{B}_2\text{O}_5:\text{xEu}^{2+}$  ( $x=1$  mol%, 3 mol%, 5 mol%, 7 mol%, 9 mol%, 11 mol%, 13 mol%) and weighed on an electronic scale. Then the raw material powders were mixed adequately in an agate mortar for 30 minutes. Thirdly, the mixtures were encased into alumina crucibles and heated successively at  $1050^\circ\text{C}$  for 2 hours in a reducing atmosphere. The reducing atmosphere was produced by burning carbon. All samples doping various  $\text{Eu}^{2+}$  concentrations were obtained under the same condition. Lastly, the samples were cooling to room temperature by naturally.

The X-ray diffraction (XRD) of the phosphors were measured by a Rigaku Ultima IV X-ray diffractometer with  $\text{Cu K}\alpha$  (40.0KV, 20.0 mA) radiation ( $\lambda=0.15406\text{\AA}$ ). The excitation and emission spectra were tested by a Japan Shimadzu RF5301PC Fluorescence Spectrophotometer equipped with a 150W Xe lamp.

### 3. Results and discussions

#### 3.1. Structure of $\text{Sr}_2\text{B}_2\text{O}_5:\text{Eu}^{2+}$ phosphor doped with different concentrations of $\text{Eu}^{2+}$ ions

Fig. 1 shows the XRD patterns of  $\text{Sr}_2\text{B}_2\text{O}_5$  phosphors doped with different concentrations of  $\text{Eu}^{2+}$  ions varying from 0.01 to 0.11 spacing 0.02. The diffraction peaks of  $\text{Sr}_2\text{B}_2\text{O}_5:\text{Eu}^{2+}$  with various concentrations is consistent with PDF card (No.73-1930), indicating that all the phosphors have the same crystal structure of monoclinic system and  $\text{P}2_1/\text{a}$  (14) space group. There are no any other diffraction peaks about  $\text{Eu}_2\text{O}_3$ , indicating that there is no mixed phase in phosphors and  $\text{Eu}^{2+}$  ions entered into the lattice of  $\text{Sr}_2\text{B}_2\text{O}_5$ . But the radius of the  $\text{Eu}^{2+}$  ion (0.109 nm) is less than the radius of the  $\text{Sr}^{2+}$  ion (0.113 nm), the diffraction angles overall enlarge a little.

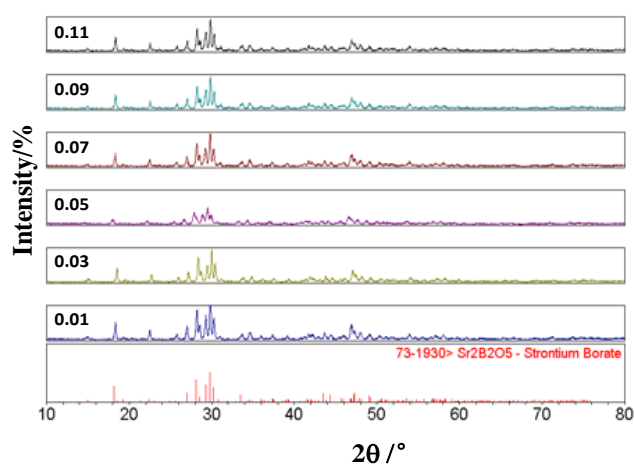


Fig. 1. XRD patterns of the samples with different  $\text{Eu}^{2+}$  ion concentrations

#### 3.2. The luminescence properties of the $\text{Sr}_{1.93}\text{B}_2\text{O}_5:0.07\text{Eu}^{2+}$ phosphor

Fig. 2 shows the fluorescent spectra of  $\text{Sr}_{1.93}\text{B}_2\text{O}_5:0.07\text{Eu}^{2+}$  phosphor. Fig. 2 (a) is the excitation spectra detected at 451 nm, 469 nm, 483 nm, 503 nm emission peak respectively, Fig. 2 (b) is the emission spectrum excited at 254 nm and 365 nm. Fig. 2 (a) shows the excitation spectra locate at UV region, and consist of a broad band from 200 nm to 264 nm and a little excitation peak at 365 nm. As can be seen from Fig. 2 (a), the phosphor can be excited efficiently from 223 nm to 264 nm. The sharp excitation edge appears at 264 nm, we think that the excitation less than 264 nm arise from the charge transfer transition of the matrix of  $\text{Sr}_2\text{B}_2\text{O}_5$ . Monitoring different luminescent peaks will conduce to understand the origin of emission peak. Result demonstrates all emission peaks come from same energy transition. From Fig. 2 (b), we can see that both of the emission spectra excited at 254 nm and 365 nm show broad asymmetric band extending from 400 nm to 700 nm and their the emission peaks

locate at 469 nm corresponding to the  $4f^65d^1$  to  $4f^7$  transition of  $\text{Eu}^{2+}$  ion. The abnormal rise of excitation after 375 nm indicates that the excitation and emission spectra will overlap, which will caused the radiation re-absorption.

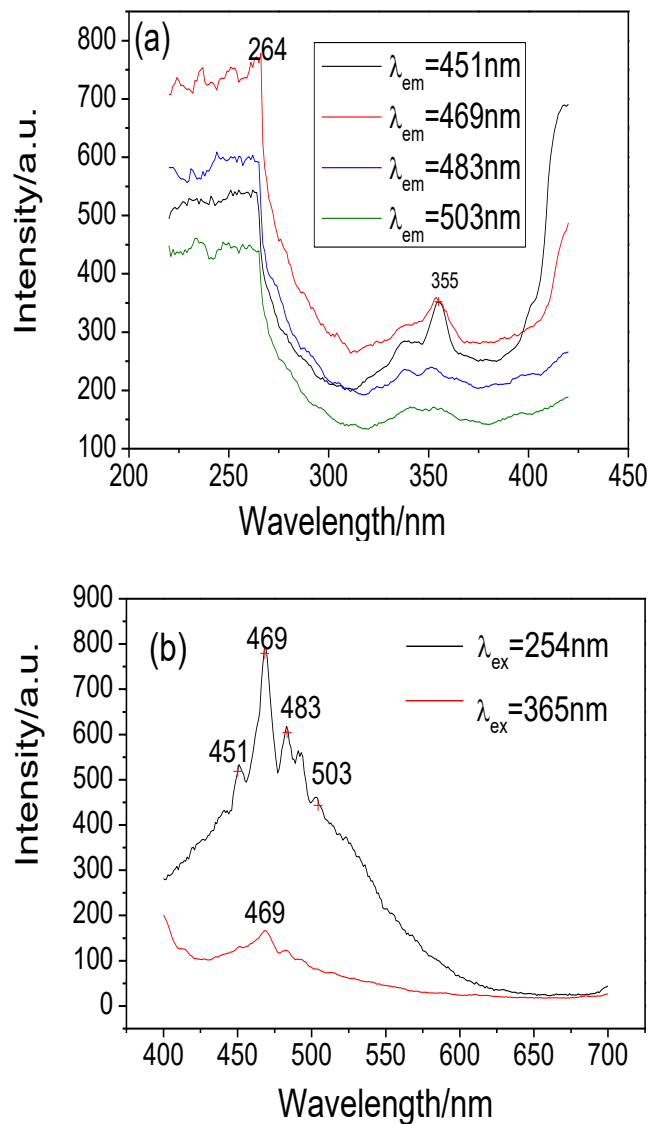


Fig. 2. The spectra of  $\text{Sr}_{1.93}\text{B}_2\text{O}_5:0.07\text{Eu}^{2+}$  samples (a) excitation spectra (b) emission spectrum

#### 3.3. The effect of $\text{Eu}^{2+}$ doping concentration on luminescence properties of $\text{Sr}_2\text{B}_2\text{O}_5:\text{Eu}^{2+}$ phosphor

Fig. 3 shows the fluorescent spectra of  $\text{Sr}_2\text{B}_2\text{O}_5:\text{xEu}^{2+}$  phosphors with different concentrations of  $\text{Eu}^{2+}$  ions varying from 0.01 to 0.13 spacing 0.02. Fig. 3 (a) shows the excitation spectrum. Fig. 3 (b) shows the emission spectrum. As can be seen from Fig. 3 (b), the emission intensity keeps increasing before the concentration of  $\text{Eu}^{2+}$  reaches 5 mol%, and then decreasing with the increase of  $\text{Eu}^{2+}$  concentration. This changing rule caused by the

quantity of luminescent centers. When  $\text{Eu}^{2+}$  concentration is less than 5 mol%, there are the little amounts of active  $\text{Eu}^{2+}$  ions, and the seldom number of luminescent centers is little, which lead to low luminescent intensity, simultaneously, the interaction of  $\text{Eu}^{2+}-\text{Eu}^{2+}$  also was restricted. Therefore, before the concentration of  $\text{Eu}^{2+}$  ions reach 5 mol%, the less the concentration is, the lower the luminescent intensity is. When  $\text{Eu}^{2+}$  ions concentration is 5 mol%, the intensities of emitting and exciting spectra reach maximum. If the amounts of  $\text{Eu}^{2+}$  ions increased continually, the interaction of  $\text{Eu}^{2+}-\text{Eu}^{2+}$  increased, the luminescence intensity decreases, and causing concentration quenching. So we thought that the optimum  $\text{Eu}^{2+}$  ions concentration of  $\text{Sr}_2\text{B}_2\text{O}_5:\text{xEu}^{2+}$  is 5 mol%. The excitation spectra in Fig. 3 (a) have the same change rule with the emission spectra. The excitation intensity firstly increased then decreased with the increasing of  $\text{Eu}^{2+}$  ions concentration.

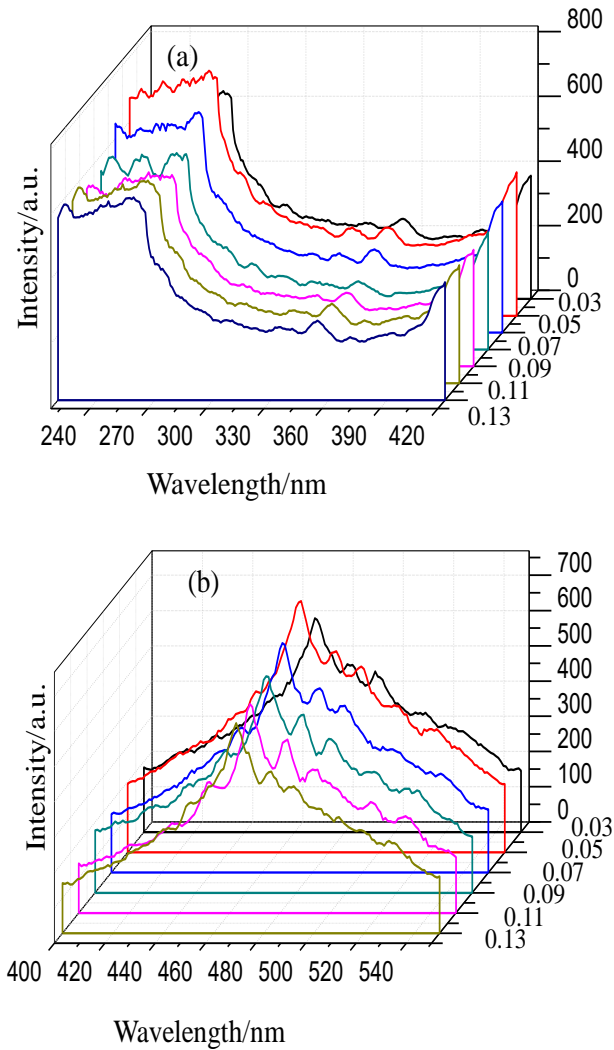


Fig. 3. The spectra of  $\text{Sr}_2\text{B}_2\text{O}_5:\text{xEu}^{2+}$  samples with various  $\text{Eu}^{2+}$  ions concentration (a) excitation spectra (b) emission spectra

In order to explain the specific reason caused the concentration quenching, Blasse [18] has pointed out that the critical transfer distance ( $R_c$ ) was approximately equal to twice the radius of a sphere with this volume:

$$R_c \approx 2 \left( \frac{3V}{4\pi x_c N} \right)^{1/3} \quad (1)$$

where  $x_c$  is the critical concentration,  $N$  is the number of cations in the unit cell and  $V$  is the volume of the unit cell. From Fig. 1, we can see that the XRD pattern of  $\text{Sr}_2\text{B}_2\text{O}_5:\text{Eu}^{2+}$  phosphor is in good agreement with JCPDS No.73-1930, in which the lattice parameter values are  $a=11.85 \text{ \AA}$ ,  $b=5.35 \text{ \AA}$ ,  $c=7.71 \text{ \AA}$ , so the unit cell volume is  $488.795 \text{ \AA}^3$ ,  $N=8$ . The optimal concentration 0.05 is used as the critical concentration  $x_c$ . Using eq. (1), the value of  $R_c$  in  $\text{Sr}_2\text{B}_2\text{O}_5:\text{Eu}^{2+}$  phosphor under 254 nm excitation is found to be  $13.26 \text{ \AA}$ .

It is known that resonance energy transfer (non-radiative energy transfer) includes exchange interaction and multipole-multipole interaction. While the typical critical distance is over  $\sim 5 \text{ \AA}$ , the concentration quenching is come from electric multipole interaction [19]. Therefore, the Dexter theory [20, 21] was introduced as formula (2) into the  $\text{Sr}_2\text{B}_2\text{O}_5:\text{xEu}^{2+}$  phosphors.

$$I/x = K \left[ 1 + \beta(\chi)^{Q/3} \right]^{-1} \quad (2)$$

Here,  $I$  is the luminescent intensity,  $K$  and  $\beta$  are constants for the same excitation condition for a given host crystal,  $x$  is the activator concentration, in our experiments,  $x$  is the concentration of  $\text{Eu}^{2+}$  ions doping in  $\text{Sr}_2\text{B}_2\text{O}_5:\text{Eu}^{2+}$ ,  $Q$  is 6, 8 or 10 for dipole-dipole, dipole-quadrupole or quadrupole-quadrupole interaction respectively. When activator ions exceed quenching concentration, the formula (2) about interaction type between sensitizers or between sensitizer and activator can be changed to formula (3).

$$\lg(I/x) = c - (Q/3) \lg x \quad (3)$$

In the phosphors, the quenching concentration starts from 5 mol%, so when the doping concentration exceeds 5 mol%, the formula (3) can be used to analysis the mechanism for concentration quenching of  $\text{Sr}_2\text{B}_2\text{O}_5:\text{Eu}^{2+}$ . According to formula (3), the plot of  $\lg(I/x)$  vs  $\lg(x)$  was drawn and shown in Fig. 4. It is clear that the plot is linear and we use the least squares method to find out the slope is  $-1.1945$ . Using formula (3), the  $Q$  value is 3.58, which is close to 6, indicating that the electric multipole interaction originated from the dipole-dipole interaction. But  $Q$  value 3.58 is also far less 6, we thought it should be ascribed to the aforementioned radiation re-absorption. Because the part  $\text{Eu}^{2+}$  ions take part in the re-absorption, it makes the electric multidipole interaction decrease, meanwhile, the effect of re-absorption on the luminescent intensity is less

than that of electric multipole, which makes luminescent intensity slow down. Therefore, the concentration quenching of the phosphor should include dipole-dipole interaction and radiation re-absorption in  $\text{Sr}_2\text{B}_2\text{O}_5:\text{Eu}^{2+}$  phosphor.

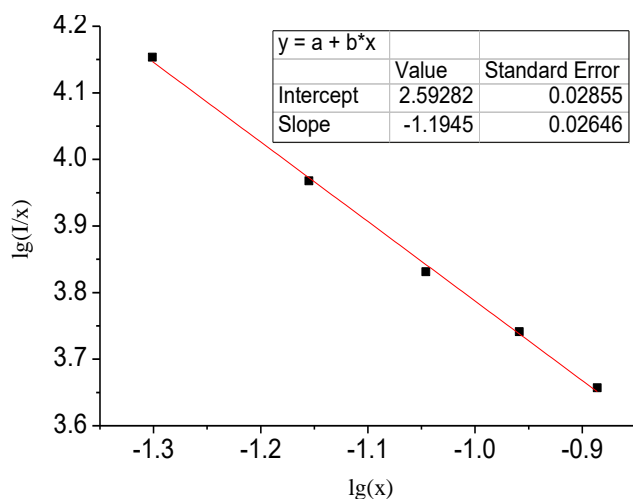


Fig. 4. The plot of  $\lg(x)$  vs  $\lg(I/x)$  in the phosphor doped  $\text{Eu}^{2+}$  from 5 mol% to 13 mol%

#### 4. Conclusions

$\text{Sr}_2\text{B}_2\text{O}_5:\text{Eu}^{2+}$  phosphors doping with various concentrations were synthesized by high-temperature solid state reaction. The crystal structure of  $\text{Sr}_2\text{B}_2\text{O}_5:\text{Eu}^{2+}$  show monoclinic system with space group of  $\text{P}2_1/\text{a}(14)$ . It does not change the crystal structure when doping  $\text{Eu}^{2+}$  ions with less than 13 mol%. The emission spectrum of the samples consists of a broad asymmetric band peaking at 469 nm under deep-ultraviolet excitation. The optimum doping concentration of  $\text{Eu}^{2+}$  ions is 5 mol%. The concentration quenching mechanism can be interpreted by the dipole-dipole interaction and radiation re-absorption of  $\text{Eu}^{2+}$  ions.

#### Acknowledgments

This work was supported by the projects of Jilin Science and Technology Bureau (No. 201201117) and of the Education Department of Jilin Province (No. JJKH20181094KJ), of innovation fund of Changchun University of Science and Technology (No.000566).

#### References

- [1] W. B. Im, Y. I. Kim, N. N. Fellows, H. Masui, G. A. Hirata, S. P. Den-Baars, R. Seshadri, *Appl. Phys. Lett.* **93**, 091905 (2008).
- [2] T. Nishida, T. Ba, N. Kobayashi, *Appl. Phys. Lett.* **82**, 3817 (2003).
- [3] J. S. Kim, P. E. Jeon, J. C. Choi, H. L. Park, S. I. Mho, G. C. Kim, *Appl. Phys. Lett.* **84**, 2931 (2004).
- [4] N. Xie, Y. Huang, X. Qiao, L. Shi, H. Seo, *Mater. Lett.* **64**, 1000 (2010).
- [5] L. Yi, X. He, L. Zhou, F. Gong, R. Wang, J. Sun, *J. Lumin.* **130**, 1113 (2010).
- [6] J. F. Xi, F. H. Zhang, Q. Mu, *Spectrosc. Spect. Anal.* **31**, 2337 (2011).
- [7] T. Murata, T. Tanoue, M. Iwasaki, K. Morinaga, T. Hase, *J. Lumin.* **114**, 207 (2005).
- [8] M. Nazarov, C. Yoon, *Solid State Chem.* **179**, 2529 (2006).
- [9] Q. S. Liu, X. Y. Zhang, Z. H. Bai, X. C. Wang, L. P. Lu, X. Y. Mi, *Spectrosc. Spect. Anal.* **29**, 769 (2009).
- [10] Y. Y. Luo, D. S. Jo, K. Senthil, S. Tezuka, M. Kakihana, K. Toda, T. Masaki, D. H. Yoon, *J. Solid State Chem.* **189**, 68 (2012).
- [11] Q. S. Liu, X. Y. Hao, G. F. Xu, L. Zhao, D. D. Cao, R. Wang, X. Y. Zhang, H. Y. Sun, *J. Inorg. Chem.* **26**, 1303 (2010).
- [12] C. K. Chang, T. M. Chen, *Appl. Phys. Lett.* **91**, 081902 (2007).
- [13] Y. M. Xue, X. W. Xu, L. Hu, Y. Fan, X. Q. Li, J. J. Li, Z. J. Mo, C. C. Tang, et al., *J. Lumin.* **131**, 2016 (2011).
- [14] D. H. Kim, J. H. Ryu, S. Y. Cho, *Appl. Phys. A.* **102**, 79 (2011).
- [15] Y. Song, Q. S. Liu, X. Y. Zhang, X. G. Fang, T. Cui, *Material Research Bulletin* **6787**, 1 (2013).
- [16] Q. S. Liu, T. Cui, X. Y. Zhang, Y. Song, *Functional Materials Letters* **6**, 1350009 (2013).
- [17] Q. S. Liu, Z. Y. Zheng, L. Q. Cheng, X. Y. Zhang, Y. Song, J. W. Liu, T. Cui, *Functional Materials Letters* **3**, 1350034 (2013).
- [18] G. Blasse, *Philips Res. Rep.* **24**, 131 (1969).
- [19] G. Blasse, *Physics Letters A* **28**, 444 (1968).
- [20] L. G. Van Uitert, *J. Electrochem. Soc.: Solid State Science* **114**, 1048 (1967).
- [21] D. L. Dexter, J. H. Schulman, *J. Chem. Phys.* **22**, 1063 (1954).

\*Corresponding author: liuqs@cust.edu.cn